Generation of Reproducible Reference Insulation Defects in Experimental Tests Cells for Controlled PD monitoring

F. Álvarez(l), F. Garnacho(2), A. Ramírez(2), E. Arcones(l), P. García(l) and C.A. Vera(l)
(l) Universidad Politécnica de Madrid. Madrid, Spain
(2) High Voltage Technological Center LCOE-FFII. Getafe (Madrid), Spain
fernando.alvarez@upm.es

***Abstract:* Partial discharge (PD) monitoring applications enable the performance of appropriate diagnosis regarding the insulation condition of high-voltage (HV) electrical grids. During the last decade on-line PD monitoring systems have been increasingly implemented by utilities and large electricity consumers in HV installations. Therefore, the evaluation of their performance is interesting in order to check whether they are generally effective with respect to their functionalities. For the characterisation of the PD monitoring instruments and of the requirements of acquisition time (number of cycles per second), the performance of laboratory tests with real insulation defects is required. As these are monitoring tests, they entail a long time (at least one day), and during this time the monitored insulation defects must behave in a stable manner. The main scope of the study presented is to design, manufacture and characterise the behaviour of three test cells, each integrating a characteristic insulation defect, with the aim of using them in laboratory monitoring tests lasting at least one day. The considered insulation defects are as follows: an internal cavity in a solid dielectric, corona effect and a surface defect. The measurements carried out with the designed test cells have shown that they are suitable for their implementation in PD monitoring tests of long duration.**

I. Introduction

The analysis of the types of defects and degradation modes in different insulation materials of HV electrical systems has shown that the presence of PD is very common in all of them. Once PD activity is detected, the identification and location of the associated type of defect is very important to evaluate whether the discharges are harmful or not.

Several PD instruments have been developed to carry out on-line monitoring measurements [1-3]. When on-line PD monitoring is performed, applying a suitable method [4-6], an expert in insulation diagnosis should be able to detect PD pulses generated by incipient insulation defects in the presence of noise disturbances, localise them, separate various PD sources present simultaneously and lastly identify them. Thus, a proper characterisation during a long period of time of PD monitoring applications is recommendable.

In various studies conducted about PD measurements, several tests samples with insulation defects were performed to test the effectiveness of a certain development and obtain experimental results from practical case studies [7, 8]. However, in very few of these studies the insulation defects were tested for long periods of time [9, 10]. Hence, the suitability of these samples to perform long-lasting monitoring measurements is not known.

In the present study, insulation defects were measured for 48 hours in order to check their suitability to be used in the realisation of long-lasting monitoring measurements. Specific insulation defects were created to generate in a controlled way various PD sources that can be combined and generated simultaneously with a voltage level lower than 20 kV. The insulation defects developed are integrated in experimental tests cells to generate PD pulses of different types for long periods of time. These test cells can then be installed in laboratory experimental setups that represent parts of real HV installations, to test or evaluate the effectiveness and improvements of monitoring applications. In these laboratory setups the insulation defects generated can be measured simultaneously and for long periods of time. The possibility of performing PD monitoring measurements with real insulation defects is interesting from both a scientific and a didactic point of view.

In Section II of this document the tests cells developed are described. In Section III the experimental setup performed to carry out the experimental tests is presented. Lastly, in Section IV the experimental measurements performed to determine the behaviour of the test cells are carried out and the results are discussed.

II. Test cells

For the design of the test cells rod electrodes with a semi-spherical end were used to generate internal PD in polyethylene, corona PD in air and surface PD also in polyethylene (see Fig. 1).

For fixed gap distances s and well-known dielectric media, electrode configurations and operating conditions (temperature, pressure and humidity), the inception voltage can be selected by choosing an appropriate curvature radius of the rod electrode. The inception voltage U_i of PD activity for an electrical configuration is given by the following equation:

The research reported here was financed from the EMPIR programme 15NRM02 UHV, which is co-funded by the European Union´s Horizon 2020 research and innovation programme and the EMPIR participating states within EURAMET.

978-1-5386-5086-8/18/$31.00 ©2018 IEEE

$$U_i = E_{dh} \cdot s \cdot \eta \qquad (1)$$

where

U_i is the inception voltage

s the gap distance

η the inhomogeneity coefficient, and

E_{dh} the breakdown electrical field for quasi-homogenous field in air, that is given by the empirical formula [11]:

$$E_{dh} = 23 \cdot \left(1 + \frac{1}{\sqrt[3]{R}}\right) \qquad (2)$$

being *R*, the curvature radius of the electrode expressed in cm to get the electrical field in kV/cm.

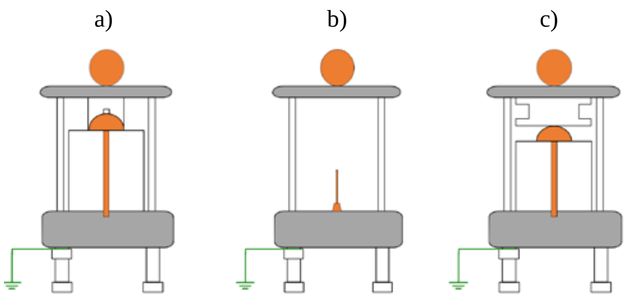

Figure 1. Layout of the test cells. a) Internal defect in polyethylene, b) corona effect in air and c) surface defect in polyethylene.

The test cell with the internal defect (see Fig. 1a) is designed with a polyethylene cylinder that has a semi-spherical hole on its base. A cavity is performed on the concave part of the sample hole to produce an internal cavity defect. The rod radius is of 7.5 mm and the dielectric thickness between both electrodes is not more than 7.5 mm. The inception voltage for this defect is 9,5 kV and the withstand voltage is higher than 35 kV.

The test cell with the corona effect (see Fig. 1b) is composed by a point-plane configuration being the plane connected to HV. The sensing electrode is a rod, which end is in the centre of the plane. In order to achieve a stable PD activity, the curve radius chosen for the rod is 1 mm and the air gap between both electrodes is 50 mm. The material recommended for the rod is tungsten. The inception voltage for this defect is 12,5 kV and the withstand voltage is higher than 25 kV.

And the test cell with the surface defect (see Fig. 1c) is designed with a dielectric sample of polyethylene that has a rotational form with a height of 54 mm and a leak line of 60 mm. This rotational sample is fixed between the HV superior electrode and the rod electrode. The inception voltage for this defect is 10 kV and the withstand voltage is higher than 25 kV.

The deviation between the calculated and experimental values for the incipient voltage of these test cells was less than 1 kV.

III. Experimental Setup

An experimental setup was implemented in a HV laboratory to evaluate the behaviour of the developed test cells, see Fig. 2. This installation was composed by the subsystems indicated in table I.

The autotransformer (1) was used to regulate the voltage level generated by the HV transformer (2). To reject the electromagnetic noise and pulsating interferences coming from the side of the HV transformer and to prevent a short cut for the PD signals generated through the HV transformer, a noise blocking impedance (3) was installed. After this blocking impedance the test cells with characteristic defects (4) were mounted on an insulator. A high frequency current transformer (HFCT) sensor (5), placed in the earth connection of the test cells, was used to measure the PD activity generated.

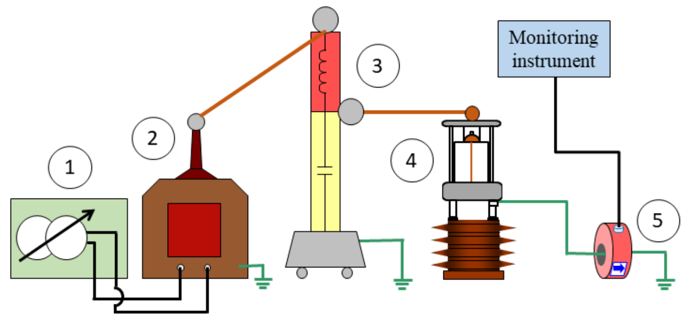

Figure 2. Experimental setup performed for the characterisation of the test cells.

TABLE I

Main components of the experimental setup

Number of element	Component of the setup
1	Autotransformer (voltage regulator) 0-250 V
2	HV transformer 110V/66kV
3	Blocking impedance
4	Test cell with a defect
5	HFCT sensor

IV. Experimental Measurements and Analysis

As it was indicated in previous section, the PD pulses generated in the dielectrics were measured with a HFCT sensor placed in the grounding connections of the test cells, see Fig. 2. The bandwidth of this sensor is from 100 kHz to 20 MHz. The monitoring instrument used is equipped with an acquisition card whose main characteristics are: 14 bits of vertical resolution, 50 MHz of bandwidth and 100 MS/s of sampling frequency.

For each individual test cell, a monitoring measurement of 48 hours was performed. The test voltage during the monitoring periods was 19 kV. A summary of the representative phase resolved PD (PRPD) patterns obtained for the internal defect, the corona effect and the surface defect are shown in Tables II, III and IV, respectively. The PRPD patterns displayed represent the PD activity registered in the first 5 minutes of each time interval of 6 hours. Furthermore, the trends over time of the PD rate (number of pulses per period) and the amplitude, for each insulation defect, are shown in Fig. 3, 4 and 5. In the graphics shown, an average value of PD rate and amplitude is depicted per each hour of the monitoring period.

TABLE II
REPRESENTATIVE PRPD PATTERNS OBTAINED FOR THE INTERNAL DEFECT

0-6 hours	**6-12 hours**	**12-18 hours**	**18-24 hours**
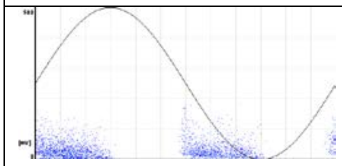	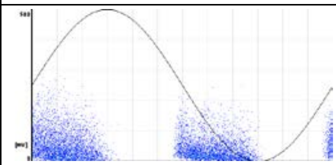	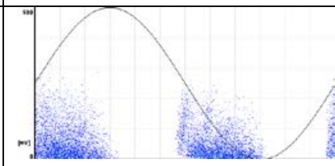	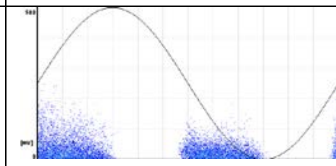
Rate: 24 PD/period Amplitude: 87 mV	Rate: 30 PD/period Amplitude: 95 mV	Rate 31 PD/period Amplitude: 94 mV	Rate: 29 PD/period Amplitude: 90 mV
24-30 hours	**30-36 hours**	**36-42 hours**	**42-48 hours**
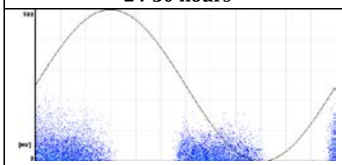	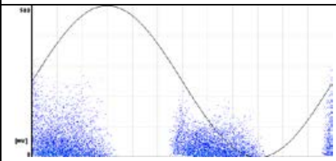	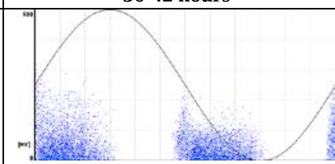	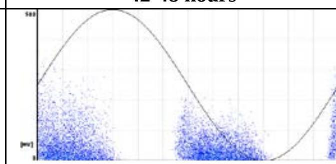
Rate: 29 PD/period Amplitude: 90 mV	Rate: 29 PD/period Amplitude:93 mV	Rate:30 PD/period Amplitude: 92 mV	Rate: 30 PD/period Amplitude: 97 mV

TABLE III
REPRESENTATIVE PRPD PATTERNS OBTAINED FOR THE CORONA EFFECT

0-6 hours	**6-12 hours**	**12-18 hours**	**18-24 hours**
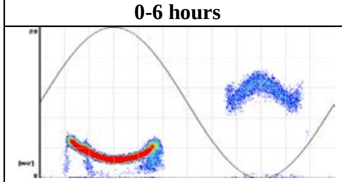	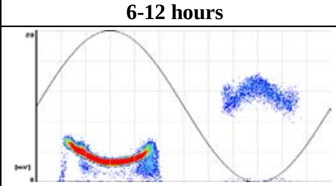	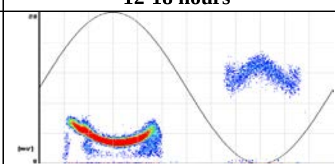	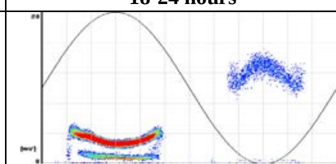
Rate: 1116 PD/period Amplitude:11,8 mV	Rate: 1082 PD/period Amplitude: 12 mV	Rate: 1071 PD/period Amplitude: 12,2 mV	Rate: 1117 PD/period Amplitude: 12,3 mV
24-30 hours	**30-36 hours**	**36-42 hours**	**42-48 hours**
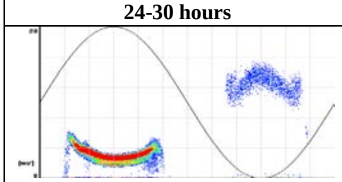	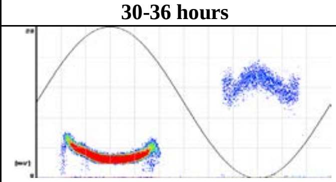	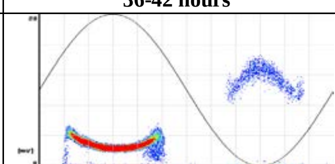	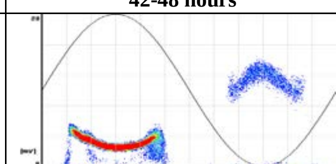
Rate: 1114 PD/period Amplitude: 12,1 mV	Rate: 1131 PD/period Amplitude: 12,5 mV	Rate: 1127 PD/period Amplitude: 12,2 mV	Rate: 1129 PD/period Amplitude: 11,9 mV

TABLE IV
REPRESENTATIVE PRPD PATTERNS OBTAINED FOR THE SURFACE DEFECT

0-6 hours	**6-12 hours**	**12-18 hours**	**18-24 hours**
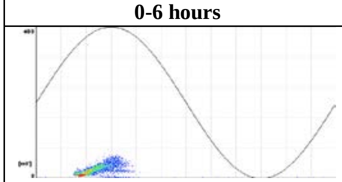	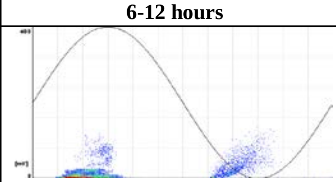	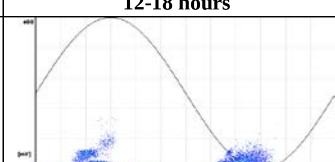	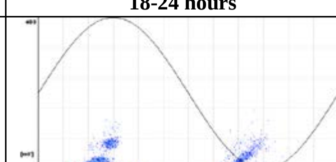
Rate: 50 PD/period Amplitude: 80 mV	Rate: 65 PD/period Amplitude: 95 mV	Rate: 60 PD/period Amplitude: 90 mV	Rate: 62 PD/period Amplitude: 100 mV
24-30 hours	**30-36 hours**	**36-42 hours**	**42-48 hours**
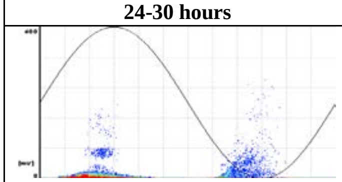	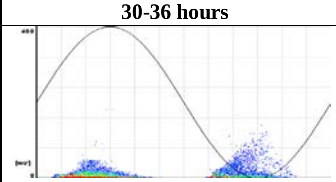	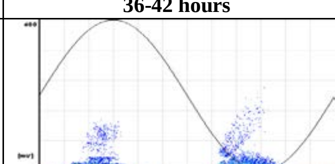	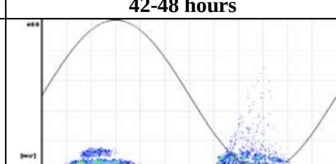
Rate: 75 PD/period Amplitude: 110 mV	Rate: 80 PD/period Amplitude: 100 mV	Rate: 77 PD/period Amplitude: 105 mV	Rate:70 PD/period Amplitude: 102mV

In the PRPD patterns shown in Tables II, III and IV, the areas with greater or lesser density of PD can be identified. The blue colours represent zones with low values of PD rate, the green and yellow areas represent intermediate values and the reddish represent the highest rates. For each represented pattern the amplitude and the average value of PD rate are indicated.

a) b)

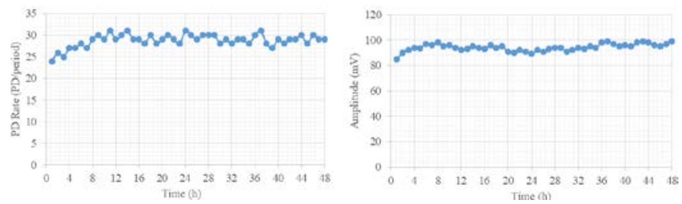

Figure 3. Internal defect. a) Trend over time of the PD rate, b) Trend over time of the PD amplitude.

a) b)

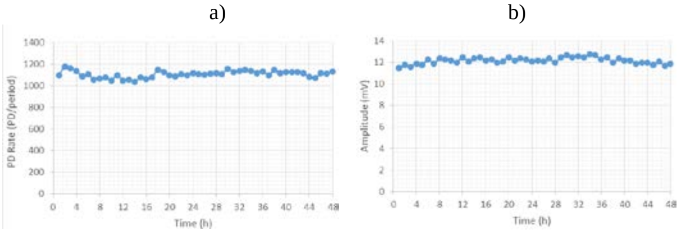

Figure 4. Corona effect. a) Trend over time of the PD rate, b) Trend over time of the PD amplitude.

a) b)

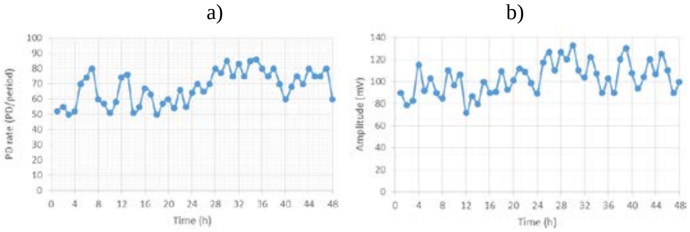

Figure 5. Surface defect. a) Trend over time of the PD rate, b) Trend over time of the PD amplitude.

For the internal defect during the 6 first hours the PD rate is slightly increasing as well as the amplitude of the pulses. After these hours the trends have been more stable.

For the corona effect, in the complete monitoring period, a stable behaviour has been obtained both in PD rate and in amplitude.

Finally, for the surface defect, although the trends in PD rate and amplitude are not so stable, it can be stated that this test cell is representative of a surface defect in the whole monitoring period of 48 hours.

Clear PRPD patterns of an internal defect, a corona effect and a surface defect have been obtained during the monitoring period of 48 hours.

V. CONCLUSIONS

The characterisation of already exiting monitoring applications or of new developments is interesting, in order to check whether they are more or less effective with respect to their functionalities. For the evaluation of these applications the realisation of long lasting laboratory tests with real insulation defects is required.

In the study presented three test cells with real insulation defects have been designed, manufactured and characterised, with the aim to be used in laboratory monitoring tests of at least one day of duration. The results obtained after 48 hours of continuing monitoring have proven the suitability of the developed test cells for their individual or combined use in laboratory measurements.

The possibility of making PD monitoring measurements with these real insulation defects results interesting not also for scientific purposes but also for didactic issues.

ACKNOWLEDGMENT

The authors thank the technical assistance from the staff of the High-Voltage Laboratory of the Universidad Politécnica de Madrid (LAT-UPM), where the practical part of this research was performed.

REFERENCES

[1] A. Cavallini, G.C. Montanari, F. Puletti and A. Contin, “A new methodology for the identification of PD in electrical apparatus: properties and applications”, IEEE Trans. Dielectr. Electr. Insul., Vol. 12, No. 2, pp. 203-215, 2005.

[2] W. Koltunowicz and R. Plath, “Synchronous multi-channel PD measurements”, IEEE Trans. Dielectr. Electr. Insul., Vol. 15, No. 6, pp. 1715-1723, 2008.

[3] F. Álvarez, F. Garnacho, J. Ortego and M.A. Sánchez-Urán, “Application of HFCT and UHF sensors in on-Line partial discharge measurements for insulation diagnosis of high voltage equipment”, Sensors Vol. 15, pp. 7360–7387, 2015.

[4] F. Álvarez, J. Ortego, F. Garnacho and M.A. Sanchez-Urán, “Advanced techniques for on-line PD measurements in high voltage systems”. International Conference on High Voltage Engineering and Application (ICHVE), Poland, 2014.

[5] F. Álvarez, J. Ortego, F. Garnacho, M.A. Sanchez-Urán and D. Prieto, “Partial discharge experiences in HV grids applying wideband measurements”. International Conference on High Voltage Engineering and Application (ICHVE), Poland, 2014.

[6] A. Kyprianou, P.L. Lewin, V. Efthimiou, A. Stavrou and G.E. Georghiou, “Wavelet packet denoising for online partial discharge detection in cables and its application to experimental field results”. Measurement Science and Technology. Vol. 17, pp. 2367-2379, 2006.

[7] A. Rodrigo, L.C. Castro, D.A. Harmsen and F.A. Muñoz, “A new design of a test platform for testing multiple partial discharge sources”, International Journal of Electrical Power and Energy Systems, Vol. 94, pp. 374-384, 2018.

[8] G. Wang, H. Jo, S.J. Kim, S. Kim and G. Kil, “Measurement and analysis of partial discharges in SF_6 gas under HVDC”. Measurement, Vol. 91, pp. 351-359, 2016.

[9] X. Zhou, H.B. Shi, M. Kuhnke, P. Werle, E. Gockenbach and H. Borsi. “Evolution and discharge pattern of creeping discharge at aged oil/pressboard interface”. IEEE Conference on Electrical Insulation and Dielectric Phenomena (CEIDP), Canada, 2016.

[10] X. Yi and Z. D. Wang. “Surface tracking on pressboard in natural and synthetic transformer liquids under AC stress”. IEEE Trans. Dielectr. Electr. Insul., Vol. 20, No. 5, pp. 1625 - 1634, 2013.

[11] E. Kuffel, W. S. Zaengl and J. Kuffel. “High Voltage Engineering: Fundamentals”. 2nd ed., Butterworth-Heinemann, 2000.